2020 Building Performance Modeling Conference and
SimBuild co-organized by ASHRAE and IBPSA-USA

OPTIMAL OPERATION FOR RESILIENT COMMUNITIES THROUGH A HIERARCHICAL LOAD SCHEDULING FRAMEWORK

Jing Wang[1], Kaitlyn Garifi[1], Kyri Baker[1], Wangda Zuo[1], Yingchen Zhang[2]
[1]University of Colorado Boulder, Boulder, CO
[2]National Renewable Energy Laboratory, Golden, CO

ABSTRACT

The increasing frequency of man-made disasters as well as extreme weather events is causing more frequent power outages. To overcome this, resilient communities with on-site photovoltaic (PV) generation and battery storage can sustain power outages and continue to operate without sacrificing the occupants' comfort needs. However, it remains challenging to prioritize and schedule the loads on a community scale during off-grid operation. This paper proposes a hierarchical load scheduling framework for the optimal operation of community loads and heating, ventilation and air-conditioning (HVAC) systems with only limited PV and batteries. The framework consists of a community coordinator layer, a building layer, and an appliance layer, which are separately formulated as rule-based resource allocation, model predictive control (MPC) problems and four types of load models. We discuss the unserved load ratio, battery sizes, PV curtailment, and thermal comfort satisfaction to evaluate the optimal load scheduling outcome. The results show the proposed framework can help maintain the community unserved load ratio at about 6.2% during the simulated 48 hours.

INTRODUCTION

The electric power grid has been faced with higher stress in the past several decades. On one hand, the increasing frequency of man-made disasters and extreme weather events is leading to more power outage events. On the other hand, the large-scale adoption of renewable energy is bringing more uncertainty and variability to the grid. It is recognized by the research community that demand side flexibility can help maintain resilience, instead of purely relying on traditional power networks for that role.

Resilience, as an emerging concept for the power grid and its connected systems, describes a system's ability to anticipate, resist, absorb, respond to, adapt to, and recover from a disturbance (Carlson et al. 2012; Wang et al. 2019). Based on this concept, a resilient community should be able to sustain disruptions (e.g., power outages), and adapt to them quickly by continuing to operate without sacrificing the comfort needs of its residents. Traditional research efforts for such resilient communities mainly focus on micro-grid formation techniques (Ding et al. 2017). In this paper, we study the problem from a building operation and load scheduling perspective.

There exist some researches for rule-based optimal operation of buildings in literature. Zhao (Zhao et al. 2013) introduced a general architecture for home energy management to reduce the energy bill cost by scheduling building loads based on electricity price signals. Zhang (Zhang et al. 2016) developed a learning-based mechanism for smart home demand response where the major home appliances are categorized into fixed, regulatable, and deferrable loads. A decoupled demand response strategy was developed with a special focus on a home HVAC system. Ayodele (Ayodele et al. 2017) used a genetic algorithm (GA) to optimally manage the critical and noncritical loads in a stand-alone PV-battery system. The results showed that adopting the load management scheme can increase the percent satisfaction of the loads. The aforementioned researches all have the scope of single buildings. The first two focused on the optimal operation while the building is still connected to the grid with an unlimited amount of power supply. However, when the community is in islanded mode, the priority of loads will change and the objective of the optimization problem also shifts. The third research studies a stand-alone PV-battery system. However, the model was nonlinear and a GA was used to solve the optimization problem, which can be computationally expensive.

Hence, to provide a general solution to optimal energy management in a community in a disaster scenario and to explore the principles of load prioritizing for resilient communities, this paper proposes a rule-based community load scheduling framework. The whole community is modeled in a hierarchical structure which consists of three layers: a community coordinator layer, a building layer and an appliance layer. As a case study, the framework is virtually tested on a community located in Anna Maria Island, FL for two consecutive days. The rest of the paper is organized as follows: Section 2 presents the methodology. Section 3 discusses the results. Section 4 concludes this paper with future work and limitations.

METHODOLOGY

Hierarchical Structure

The community load scheduling framework has a hierarchical structure as shown in Fig. 1. The top level represents the community-level where the coordinator decides how to best allocate the resources (e.g., PV energy) to each building to achieve the objective of the whole community. The middle level represents the building agents in the community, which receive signals from the coordinator and try to meet their own objective with the given resources by scheduling its appliances and battery operation. Ideally, the community coordinator should determine the resource allocation by running a community level optimization (i.e., outer-loop optimization) and then each building runs its own optimization (i.e., inner-loop optimization). In this paper, we simplified the top level to rule-based resource allocation. The building agents are implemented as independent MPC problems. Each building has its own battery. At the bottom level, we model the battery operation, HVAC system, and appliance loads. Appliance loads are categorized into four types: sheddable, modulatable, shiftable and critical and modeled separately. The following introduces each layer in detail.

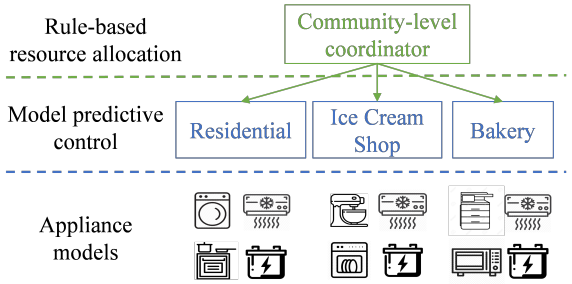

Figure 1: Hierarchical optimization framework.

Community Coordinator

The community coordinator allocates energy resources to achieve the community-level optimum. When disconnected from the main grid during outages, the only energy source is the PV power generated from on-site PV panels. In this paper, the community coordinator adopts a rule-based allocation and distributes the total PV power based on each building's maximum power demand (Scenario 1) or average power demand (Scenario 2). Thus, the allocation factor is the fraction of the total community PV power that each building is allocated. In the case study, three buildings of different types are selected to showcase the proposed framework: a residential building (area: 93.8 m^2), an ice cream shop (area: 160.5 m^2), and a bakery (area: 410 m^2). The ice cream shop has the largest power demand due to its refrigeration equipment. Table 1 lists the allocation factors used in Scenarios 1 and 2.

Table 1: PV power allocation factors

	Residential	**Ice Cream Shop**	**Bakery**
Max. Power [kW]	0.369	6.244	6.099
Scenario 1	0.029	0.491	0.48
Avg. Power [kW]	0.131	5.418	3.894
Scenario 2	0.014	0.574	0.412

Building Agents

At the building level, each building agent is formulated as an MPC problem. The optimization makes the best decision for the current time horizon based on knowledge of future predicted outdoor dry-bulb temperature, PV generation and solar radiation in order to minimize curtailment of PV generation, and continues to the next time step in a receding horizon control-based fashion. This work does not consider the uncertainty on the future predictions described above. Since the total simulation time is 48 hours, the MPC prediction horizon is selected as 12 hours with a simulation time step of one hour. This selection considers the trade-off between the simulation time and the information fed to the optimizer. The optimization objective is to maximize the PV power used while satisfying occupants' needs as much as possible over the two day simulation. To achieve this, each building has a battery for enabling energy usage to be shifted to times when there is no PV generation. Additionally, building loads can be scheduled based on occupants' preferences. The HVAC system will pre-cool the building when surplus PV power is available. To ensure thermal comfort for occupants, temperature upper and lower bounds are set according to the ASHRAE standard (ASHRAE 2017). Therefore, the optimization variables include: PV curtailment, charging and discharging power of the battery, HVAC system power, and building load power. The mathematical formation of the problem is introduced throughout the remainder of this section. Note that the following formation is applied to each building of the community.

For each of the three studied buildings, the power balance that must be satisfied at each time step is given by:

$$P^t_{PV} - P^t_{curt} = P^t_{ch} - P^t_{dis} + P^t_{load} + P^t_{HVAC}, \qquad (1)$$

where PV curtailment is limited by how much PV generation is available:

$$\text{s.t.} \quad 0 \le P^t_{curt} \le P^t_{PV}. \qquad (2)$$

In Eq. (1), P^t_{load} represents all building loads other than

the HVAC system load. The following subsections introduce the HVAC, load, and battery models in detail.

The optimization objective is to maximize the amount of PV power generation that is used or stored. In the implementation, we maximized the right-hand side of Eq. (1). Since the available PV generation P^t_{PV} is given by real data, this implementation is equivalent to minimizing P^t_{curt}. Additionally, to avoid simultaneous charging and discharging of the battery in the simulation, we added a slight penalization, α (usually a small number such as 0.01), on battery charging in the objective function reflected by Eq. (3). The objective function is given by:

$$\max \sum_{t=k}^{k+H} (P^t_{ch} - P^t_{dis} + P^t_{load} + P^t_{HVAC}) - \alpha P^t_{ch}, \quad (3)$$

where $k \in \{1,2,...,48\}$. The above and the following equations apply to every time step of the simulation.

HVAC Models

To preserve the linearity of the optimization problem, the HVAC models of the three buildings are trained using linear regression. The room temperature of the current time step is dependent on the ambient (i.e., outdoor) temperature, room temperature, HVAC cooling power, and the solar radiation through windows of past time steps. Common practice in load scheduling research is to use only one past time step (Jin et al. 2017; Garifi et al. 2018). In this paper, we adopted two past terms to better reflect the impact of building thermal mass on indoor air temperature evolution (Zakula, Armstrong, and Norford 2014). The mathematical formulation of the linear HVAC model is given by:

$$\begin{aligned} T^t_{room} =& \beta_1 T^{t-1}_{amb} + \beta_2 T^{t-2}_{amb} + \beta_3 T^{t-1}_{room} + \beta_4 T^{t-2}_{room} \\ &+ \beta_5 P^{t-1}_{HVAC} + \beta_6 Q^{t-1}_{sol} + \beta_7 Q^{t-2}_{sol} \end{aligned} \quad (4)$$

$$T_{min} \leq T^t_{room} \leq T_{max}, \quad (5)$$

where the lower and upper temperature limits are governed by ASHRAE Standard 55-2017 (ASHRAE 2017), which recommends the temperature range for thermal comfort to be approximately between 67°F and 82°F (20°C to 28°C). Thus, T_{min} is 20°C and T_{max} is 28°C.

The training data of the HVAC models are the simulation results of the corresponding physics-based HVAC system models built in Modelica (The Modelica Association 2019; He et al. 2016). The simulations were run for the entire month of August 2017 which corresponds to the hurricane season in Florida. The physics-based HVAC models were built based on system design data. The weather file embedded in the model is typical meteorological year (TMY) data for the weather station at Tampa International Airport (NREL 2019). The solar radiation data was calculated based on the direct and diffused horizontal irradiation data collected on site. The dataset has a time step of one hour and it is randomly divided into a 70:30 split for the training and the testing sets, respectively, for the linear regression model. Table 2 lists the linear regression coefficients of the three buildings, as well as the Root Mean Square Error (RMSE) to measure the accuracy of the models. The HVAC models can predict the room temperature with RMSE between 0.2°C-0.3°C.

Table 2: HVAC linear regression model coefficients

		Residential	Ice Cream Shop	Bakery
Coefficients	T^{t-1}_{room}	1.540	1.640	1.599
	T^{t-2}_{room}	-0.543	-0.645	-0.603
	T^{t-1}_{amb}	0.0541	0.0402	0.0348
	T^{t-2}_{amb}	-0.0469	-0.0348	-0.0309
	P^{t-1}_{HVAC}	-0.0310	-0.0962	-0.0810
	Q^{t-1}_{sol}	-0.176	0.197	0.112
	Q^{t-2}_{sol}	0.113	-0.211	-0.0423
RMSE [°C]		0.303	0.236	0.202

Load Models

To better schedule various building loads, they are categorized into four types based on the assumed occupants' preference during disaster circumstances, as well as the electrical characteristics of different appliances. In this paper, only loads that are related to visual comfort (e.g., lighting) and food preservation (e.g., refrigerator) are considered critical. Sheddable loads are those can be fully disconnected without impacting life quality during the studied time period. Whether a load is sheddable is determined from the building owner's aspect. For instance, the coffee maker and the soda dispenser in the ice cream shop are classified as sheddable during the outage. Modulatable loads are those have varying power amplitudes such as mixers with variable speed options. Since some plug loads in the dataset are unspecified, we sum those loads into one modulatable load. Shiftable loads are those that need to be operated but are rather flexible concerning the time of day they are scheduled. Washer, dryer, and range are considered shiftable loads in this work. Due to the disaster circumstances, some loads commonly categorized as critical are considered to be sheddable (e.g., computer) in this paper. Table 3 summarizes all load types in the three studied buildings.

Next, the mathematical models for the four types of loads are introduced. The sum of the loads across all types, P^t_{load}, is given by:

$$P^t_{load} = \sum_{a=1}^{A} P^t_{T1,a} + \sum_{b=1}^{B} P^t_{T2,b} + \sum_{c=1}^{C} P^t_{T3,c} + \sum_{d=1}^{D} P^t_{T4,d}. \quad (6)$$

Table 3: Summary of load types in studied buildings

	Residential	**Ice Cream Shop**	**Bakery**
Type 1: Sheddable	Computer	Coffee maker, soda dispenser, outdoor ice storage	Microwave
Type 2: Modulatable	HVAC	HVAC	Mixer, unspecified room plugs, HVAC
Type 3: Shiftable	Range, washer, dryer	None	Range, oven, dishwasher
Type 4: Critical	Lights, refrigerator	Lights, cooler, display case	Lights, cooler, display case

Sheddable, modulatable, and critical loads are described by:

$$P^t_{T1,a} = u^t_a * P^t_a, \quad a \in \{1,...,A\} \tag{7}$$

$$0 \le P^t_{T2,b} \le P^t_b, \quad b \in \{1,...,B\} \tag{8}$$

$$P^t_{T4,d} = P^t_d, \quad d \in \{1,...,D\}. \tag{9}$$

In Eq. (7), the actual power of a Type 1 sheddable load $P^t_{T1,a}$ equals to the original power demand P^t_a multiplied by a binary optimization variable u^t_a. Thus, the optimization will determine the ON/OFF status of the sheddable loads. The power demand data, P^t_a, is collected from power meters installed in these buildings. In Eq. (8), the actual power of a Type 2 modulatable load $P^t_{T2,b}$ is an optimization variable which determines how much of the load is modulated between zero (all) and the original power demand (none). For Type 4 critical loads, the actual power should be exactly equal to the original power demand data, as in Eq. (9).

For Type 3 shiftable loads, the scheduling matrix method introduced in Zhao's work is adopted (Zhao et al. 2013). First, using the metered power data, we extracted the average cycle time n_c and average power demand $P_{c,avg}$ for each Type 3 load. Within an optimization horizon, when the starting time of the load is determined, the power shape of this load is then fixed. Hence, the optimization variable for Type 3 loads is its starting time $t_{c,s}$, which is an integer variable. To formulate the problem, we use a series of binary variables v^t_c to indicate the starting time step. The relationship between $t_{c,s}$ and v^t_c is given by:

$$v^t_c = \begin{cases} 1, & t = t_{c,s} \\ 0, & t \ne t_{c,s} \end{cases}, \quad \forall t \in \{k,...,k+H-n_c\}, \quad c \in \{1,...,C\}. \tag{10}$$

Over the whole optimization horizon, v^t_c=1 only at the starting time step and the appliance must finish its cycle before this horizon ends ($t \in \{k,...,k+H-n_c\}$). In this paper, we assume that each shiftable load operates once and only once in each horizon, which is enforced by:

$$\sum_{t=k}^{k+H-n_c} v^t_c = 1. \tag{11}$$

Next, a scheduling matrix S_c of shape $H \times (H-n_c+1)$ is generated for each Type 3 load. The actual power shape of load c, denoted $P^t_{T3,c}$, is calculated by:

$$P^t_{T3,c} = S_c \times \begin{bmatrix} v^k_c \\ \vdots \\ v^{k+H-n_c}_c \end{bmatrix} \times P_{c,avg} \tag{12}$$

For example, when $n_c = 3$, an appliance scheduling matrix of shape 12×10 is generated as follows.

$$S_c = \begin{bmatrix} 1 & 0 & & 0 & 0 \\ 1 & 1 & & 0 & 0 \\ 1 & 1 & & 0 & 0 \\ 0 & 1 & & 0 & 0 \\ \vdots & 0 & \cdots & \vdots & 0 \\ 0 & \vdots & & 0 & \vdots \\ 0 & 0 & & 1 & 0 \\ 0 & 0 & & 1 & 1 \\ 0 & 0 & & 1 & 1 \\ 0 & 0 & & 0 & 1 \end{bmatrix} \tag{13}$$

Battery Models

In this work, we assume that each building has its own battery. The battery models are linear with separate variables for charging and discharging and include constraints on maximum charging and discharging power. The battery model is given by:

$$E^{t+1}_{bat} = E^t_{bat} + \eta_{ch} P^t_{ch} \Delta t - \frac{1}{\eta_{dis}} P^t_{dis} \Delta t \tag{14}$$

$$0 \le P^t_{ch}, P^t_{dis} \le P_{max} \tag{15}$$

$$0 \le E^t_{bat} \le E_{max}. \tag{16}$$

where $\eta_{ch} = \eta_{dis} = 0.9$. The size of each battery E_{max} is chosen such that the size will not be binding for storing PV power generation. The maximum charging/discharging power P_{max} is determined as 40% of the battery capacity. The initial battery state of charge is assumed to be 50% of E_{max}.

Hence, based on the above discussion, the optimization variables are collected in the vector:

$$x^t = [\{P^t_{curt}\}^{k+H}_{t=k}, \{P^t_{ch}\}^{k+H}_{t=k}, \{P^t_{dis}\}^{k+H}_{t=k}, \{P^t_{HVAC}\}^{k+H}_{t=k}, \{u^t_a\}^{k+H}_{t=k}, \{P^t_{T2,b}\}^{k+H}_{t=k}, \{v^t_c\}^{k+H-n_c}_{t=k}]. \tag{17}$$

RESULTS AND DISCUSSIONS

To evaluate the proposed community load scheduling framework, a case study has been implemented for a community located in Anna Maria Island, Florida during the hurricane season on August 4 and 5. Three buildings of various types have been chosen for the simulation (i.e., residential, ice cream shop, bakery) to encapsulate all four types of loads. The data inputs for the simulation (e.g., PV power, outdoor dry-bulb temperature, solar radiation) were extracted from the community physics-based model in Modelica (The Modelica Association 2019; He et al. 2016). It's noted that the simulation results shown below are directly gained from the MPC problems themselves, rather than from the detailed Modelica models. Two scenarios were designed to compare different resource allocation methods: In Scenario 1, the coordinator allocates PV power according to the maximum power demand of each building, and in Scenario 2 the allocation is based on average power demand. The community load scheduling framework is implemented as a mixed integer linear program in Python and solved using an academic Gurobi license (Gurobi 2019). The simulation results are discussed through selected key performance indices (KPIs), i.e., unserved load ratio, battery size, PV curtailment ratio, and comfort hour ratio.

Building Loads

The original load shapes before and after scheduling (for both Scenario 1 and Scenario 2) for each of the three buildings are shown in Figs. 2 to 4. The original load profiles are exported from the high-fidelity Modelica models with a room temperature setpoint of 24°C. From these figures, notice that the residential building has a much smaller power demand compared to the ice cream shop and the bakery, where a large proportion of the demand is for refrigeration. In the residential building, the HVAC load accounts for the largest proportion. In Figure 2 for Scenario 1, due to the lack of PV power, the HVAC load is slightly reduced and the shiftable loads are shifted from the night to the morning and afternoon hours. In Scenario 2, the residential HVAC load is further reduced. In the ice cream shop and the bakery, the HVAC load shapes show a different trend than in the residential building. As seen in Figs. 3 and 4, the HVAC system operates twice in the day, once in the morning and once in the afternoon. It tends to pre-cool the building when there is still PV power available and then remains off for several hours until its next operation. Hence, the original HVAC load profile tends to be flatter, compared to the scheduled HVAC load shape which has a larger amplitude. This is because the pre-cooling energy is stored in the thermal mass of the building to assure thermal comfort for later. Lastly, when PV power is not available, all critical loads and part of the sheddable and modulatable loads are served by the battery.

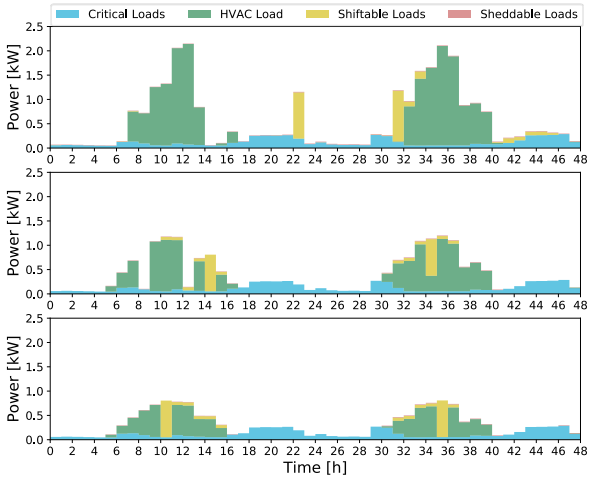

Figure 2: Residential building load profile. (Top) Original load profile. (Middle) Scenario 1 load profile. (Bottom) Scenario 2 load profile.

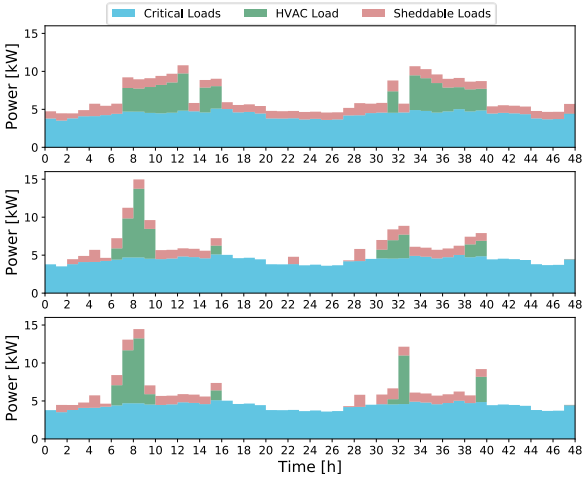

Figure 3: Ice cream shop load profile. (Top) Original load profile. (Middle) Scenario 1 load profile. (Bottom) Scenario 2 load profile.

Table 4 shows the unserved load ratio of different load types in each building, as well as in the whole community, for Scenarios 1 and 2. From Table 4, we show that all critical loads are satisfied. In the residential building, 54.4% of the sheddable loads and 19.92% of the shiftable loads are unserved in Scenario 1. In Scenario 2, the unserved sheddable load ratio increases slightly to 54.81% since less PV power is allocated to this building. The shiftable load unserved ratio is the same across both scenarios because shiftable loads operate once and only once, as described by Eq. (11). The unserved load ratio of sheddable loads of the ice cream shop increased slightly by 0.13% from Scenario 1 to 2 while more PV is allocated to this building in Scenario 2. This is likely because the optimization objective is to maximize PV

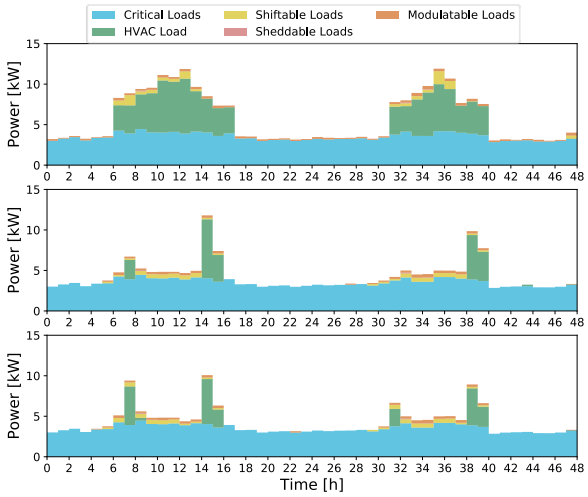

Figure 4: Bakery load profile. (Top) Original load profile. (Middle) Scenario 1 load profile. (Bottom) Scenario 2 load profile.

power usage, so it was optimal to charge the battery to serve more loads later in the prediction horizon, instead of satisfying the immediate load demand. This is also seen in the required battery size for the ice cream shop in both scenarios, which will be discussed in the next section. The unserved load ratio of modulatable loads in the bakery slightly increased in Scenario 2 since less PV is allocated. The unserved load ratio for sheddable and shiftable loads remains the same. Overall, the unserved load ratio of the whole community is at about 6.2%. However, the change of the allocated PV power in Scenario 1 and 2 is reflected in the required battery size which will be discussed next.

Power Balance and Battery Behavior

The power balance in the three buildings is depicted in Figs. 5 to 7. For the residential building, the optimization results in Fig. 5 show that the battery seldom charges with PV power. Instead, the PV is mainly used for the HVAC load to cool the building. This likely due to the relatively small total load of the residential building compared to the ice cream shop and bakery. However, for the ice cream shop and bakery results shown in Figures 6 and 7, the battery is used to store PV power from during the day for use later. In both the ice cream shop and the bakery, the HVAC is used for cooling in the morning and afternoon hours in order to charge the battery as much as possible with PV power. In the afternoon hours when the battery is almost full and the room temperature approaches the upper comfort limit, the HVAC system begins to pre-cool the building. At night, the battery discharges to serve the critical loads and partially serve the other loads. For all buildings and all scenarios, PV power is either consumed or charged into the battery; thus, none is curtailed.

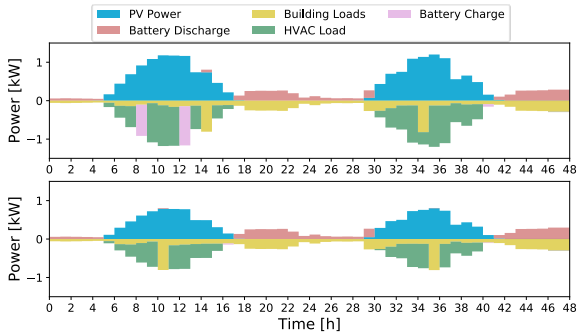

Figure 5: Residential building power balance. (Top) Scenario 1. (Bottom) Scenario 2.

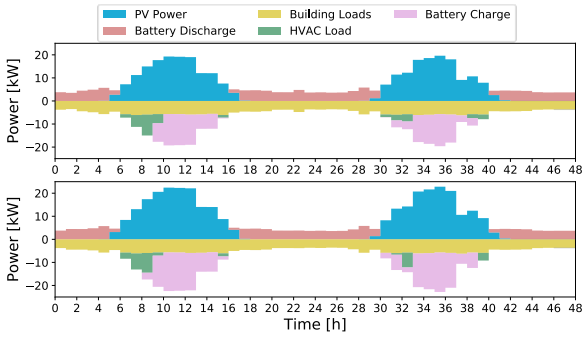

Figure 6: Ice cream shop power balance. (Top) Scenario 1. (Bottom) Scenario 2.

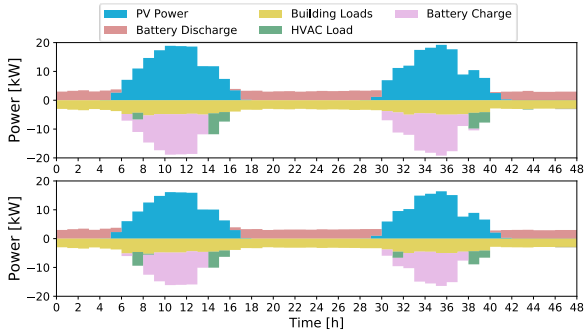

Figure 7: Bakery power balance. (Top) Scenario 1. (Bottom) Scenario 2.

Table 5 lists the minimum required battery sizes for different buildings. The sizes were calculated by subtracting the minimum battery state of charge (SOC), measured in kWh, from the maximum SOC in the simulation results. Comparing Scenario 1 with Scenario 2, the required battery size of the residential building increases despite of the reduced PV power. This was caused by more battery discharging due to the lower allocation factor in Scenario 2, which leads to a lower minimum SOC. Hence, a larger battery size is required. The required battery capacity for the ice cream shop increases in Scenario 2 in order to store more PV power since the PV allocation is greater. Similarly for the bakery, when the available PV power is greater, the required battery size is larger. This is because greater PV power availability

Table 4: Unserved load ratio of different load types

		Unserved Load Ratio				
Scenario	**Building**	**Sheddable**	**Shiftable**	**Modulatable**	**Critical**	**Overall**
1	Residential	54.40%	19.92%	N/A	0	9.01%
	Ice Cream Shop	43.11%	N/A	N/A	0	8.62%
	Bakery	1.29%	8.18%	40.56%	0	2.60%
	Community	42.97%	10.94%	40.56%	0	6.16%
2	Residential	54.81%	19.92%	N/A	0	9.04%
	Ice Cream Shop	43.24%	N/A	N/A	0	8.65%
	Bakery	1.29%	8.18%	40.59%	0	2.61%
	Community	43.10%	10.94%	40.59%	0	6.18%

Table 5: Battery size and PV curtailment

Scenario	**Building**	**Battery Size [kWh]**	**PV Curtailment Ratio**
1	Residential	3.68	0
	Ice Cream Shop	61.00	0
	Bakery	92.73	0
	Community	157.41	0
2	Residential	4.01	0
	Ice Cream Shop	92.9	0
	Bakery	56.91	0
	Community	153.82	0

leads to more charged power into the battery. As a result, the maximum battery SOC will be larger.

It should be noted that the optimization results shown here are sensitive to the battery capacity E_{max} and the maximum charging/discharging power P_{max}. Specifically, if the battery capacity constraint is binding in the optimization, the extra PV generation will be curtailed because the battery is full, causing there to be both PV curtailment and unserved load. Similarly, if the available PV generation is more than the sum of the load and battery charging limit P_{max}, there will also be PV curtailment. Increasing either of these two parameters will decrease the PV curtailment and possibly reduce the unserved load ratio and increase thermal comfort. In this paper, we sized the battery to ensure the capacity constraint was non-binding in order to investigate the battery size needed for the community to be resilient.

Thermal Comfort

The indoor and outdoor temperature during the simulation for each building are shown in Figs. 8 to 10. Additionally, a baseline temperature trajectory is plotted for reference. The baseline curve is the simulated indoor temperature without MPC by the Modelica models with a fixed setpoint of 24°C. Figs. 8 to 10 show that the temperatures of the three buildings are well maintained between 20°C and 28°C for both scenarios with the allocated PV power. For the residential building and the bakery, the indoor temperature is well maintained using the HVAC during the day, and then drifts during the nighttime hours when there is no PV generation. For the ice cream shop, the room temperature in both scenarios is maintained close to the lower thermal comfort bound of 20°C. Additionally, the ice cream shop indoor temperature decreases drastically at 8 am in the morning to about 20°C and then maintains almost unchanged because of thermal mass and another cooling provided at 3 pm.

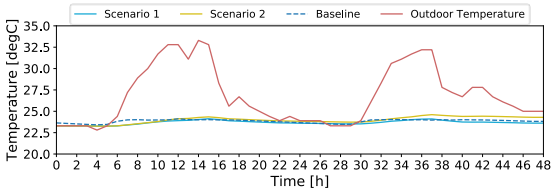

Figure 8: Residential building indoor and outdoor temperature.

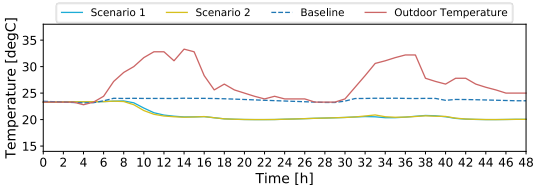

Figure 9: Ice cream shop indoor and outdoor temperature.

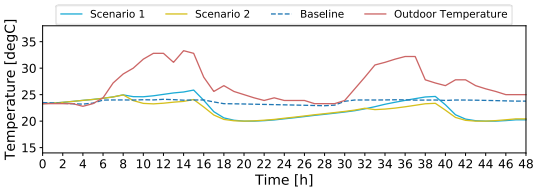

Figure 10: Bakery indoor and outdoor temperature.

CONCLUSION

In this paper, a hierarchical community load scheduling framework is proposed. KPIs such as unserved load ratio, battery size, PV curtailment and comfort hour ratio for scenarios with different PV allocation methods are

compared. Based on the analysis of the simulation results, the unserved load ratio of the whole community is at about 6.2%. For the proposed frame, the optimization results are sensitive to the battery size constraint and the maximum charging/discharging power constraint, which will be investigated in future work. Future directions also include formulating the outer-loop community level coordinator as an MPC problem to ensure the resources of different buildings could be shared dynamically, which builds upon our current static rule-based resource allocation approach used in this work.

ACKNOWLEDGMENT

This research was supported by the National Science Foundation under Awards No. OAC-1638336 and IIS-1802017.

NOMENCLATURE

Parameters and Variables

x	Vector of optimization variables
P	Power
t	Time step
H	Optimization horizon
T	Temperature
β_i	Coefficients of the HVAC model
Q	Heat flow
u, v	Binary variables for ON/OFF load status
n	Average time steps of run cycle
S	Scheduling matrix
E	Energy
η	Efficiency

Subscripts

amb	Ambient outdoor temperature
sol	Solar irradiance
$curt$	PV curtailment
ch	Battery charging
dis	Battery discharging
$HVAC$	HVAC cooling
$load$	Building loads
bat	Battery
min	Minimum value
max	Maximum value
$T1, a$	Type 1 load $a \in \{1, \ldots, A\}$
$T2, b$	Type 2 load $b \in \{1, \ldots, B\}$
$T3, c$	Type 3 load $c \in \{1, \ldots, C\}$
$T4, d$	Type 4 load $d \in \{1, \ldots, D\}$

REFERENCES

ASHRAE. 2017. ASHRAE Standard 55 (2017) - Thermal Environmental Conditions for Human Occupancy.

Ayodele, T.R., A.S.O. Ogunjuyigbe, K.O. Akpeji, and O.O. Akinola. 2017. "Prioritized rule based load management technique for residential building powered by PV/battery system." *Engineering Science and Technology, an International Journal* 20 (3): 859–873.

Carlson, J.L., R.A. Haffenden, G.W. Bassett, W.A. Buehring, M.J. Collins III, S.M. Folga, F.D. Petit, J.A. Phillips, D.R. Verner, and R.G. Whitfield. 2012. "Resilience: Theory and Application." Technical Report, Argonne National Laboratory, Argonne, IL, USA.

Ding, T., Y. Lin, G. Li, and Z. Bie. 2017. "A new model for resilient distribution systems by microgrids formation." *IEEE Transactions on Power Systems* 32 (5): 4145–4147.

Garifi, K., K. Baker, B. Touri, and D. Christensen. 2018, Aug. "Stochastic Model Predictive Control for Demand Response in a Home Energy Management System." *2018 IEEE Power Energy Society General Meeting (PESGM)*. 1–5.

Gurobi. 2019. Gurobi Optimization.

He, D., S. Huang, W. Zuo, and R. Kaiser. 2016. "Towards to the development of virtual testbed for net zero energy communities." *Proceedings of SimBuild* 6, no. 1.

Jin, X., K. Baker, D. Christensen, and S. Isley. 2017. "Foresee: A user-centric home energy management system for energy efficiency and demand response." *Applied Energy* 205:1583 – 1595.

NREL. 2019. National Solar Radiation Data Base 1991- 2005 Update: Typical Meteorological Year 3.

The Modelica Association. 2019. Modelica.

Wang, J., W. Zuo, L. Rhode-Barbarigos, X. Lu, J. Wang, and Y. Lin. 2019. "Literature review on modeling and simulation of energy infrastructures from a resilience perspective." *Reliability Engineering & System Safety* 183:360–373.

Zakula, T., P.R. Armstrong, and L. Norford. 2014. "Modeling environment for model predictive control of buildings." *Energy and Buildings* 85:549 – 559.

Zhang, D., S. Li, M. Sun, and Z. O'Neill. 2016. "An optimal and learning-based demand response and home energy management system." *IEEE Transactions on Smart Grid* 7 (4): 1790–1801.

Zhao, Z., W.C. Lee, Y. Shin, and K.-B. Song. 2013. "An optimal power scheduling method for demand response in home energy management system." *IEEE Transactions on Smart Grid* 4 (3): 1391–1400.